



**TECHNICAL  
RESEARCH  
REPORT**

AD 29939

**THE STUDY OF THE INTERACTION OF  
INTENSE PICOSECOND LIGHT PULSE  
WITH MATERIALS**

**A QUARTERLY TECHNICAL REPORT**

**SUBMITTED TO**

**THE U.S. ARMY RESEARCH OFFICE**

**PERIOD**

**March 22, 1971 to June 21, 1971**

**REPORTED BY**

**CHI H. LEE**

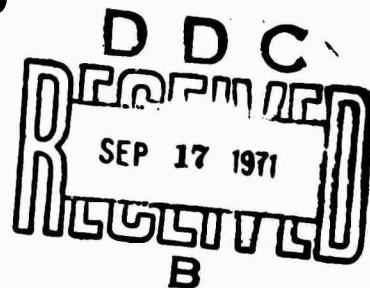
**Approved for Public Release  
Distributions Unlimited**

**DEPARTMENT OF  
ELECTRICAL ENGINEERING**

**UNIVERSITY OF MARYLAND**

**COLLEGE PARK, MARYLAND 20742**

**Reproduced by  
NATIONAL TECHNICAL  
INFORMATION SERVICE  
Springfield, Va. 22151**



216

**BEST  
AVAILABLE COPY**

Unclassified  
Security Classification

Mar 7, 66

## DOCUMENT CONTROL DATA - R &amp; D

(Security classification of title, body of abstract and indexing annotation must be entered when the overall report is classified)

1. ORIGINATING ACTIVITY (Corporate author) Department of Electrical Engineering University of Maryland College Park, Maryland 20742		2a. REPORT SECURITY CLASSIFICATION Unclassified	
3. REPORT TITLE The Study of the Interaction of Intense Picosecond Light Pulse with Material (Berg-Barrett X-ray Observation of Annealing and Laser Induced Induced Damage in Zinc.		2b. GROUP	
4. DESCRIPTIVE NOTES (Type of report and inclusive dates) A quarterly technical report, March 22 to June 21, 1971			
5. AUTHOR(S) (First name, middle initial, last name) C. Cm Wu, C. H. Lee and R. W. Armstrong			
6. REPORT DATE July 21, 1971		7a. TOTAL NO. OF PAGES 10	7b. NO. OF REFS 17
8a. CONTRACT OR GRANT NO. DA-ARO-D-31-124-71-155		8b. ORIGINATOR'S REPORT NUMBER(S)	
9. PROJECT NO. ARPA Order No. 675 Am. 9			
c. Program Code No. 9E20		9d. OTHER REPORT NO(S) (Any other numbers that may be assigned this report)	
10. DISTRIBUTION STATEMENT Reproduction in whole or in part is permitted for any purpose of the United States Government.			
11. SUPPLEMENTARY NOTES		12. SPONSORING MILITARY ACTIVITY ARPA and U.S. Army Research Office	

## 3. ABSTRACT

The Berg-Barrett x-ray diffraction contrast technique has been utilized to study the process of laser induced damage in a zinc crystal and, also to make observations on the annealing characteristics of the dislocation substructure before and after the laser treatment. Annealing caused individual dislocations to become segmented with various sections of their line lengths becoming parallel to  $\langle 10\bar{1}0 \rangle$ . This preference for a crystallographic orientation of the dislocations seemed related to the equally important observation that the subboundary "lineage" structure of the crystals was also largely composed of tilt boundaries of  $\{10\bar{1}0\}$  and  $\{11\bar{2}0\}$  surfaces. The laser induced damage required a threshold energy which caused melting, possible vaporization and appreciable plastic deformation of the matrix material by deformation twinning, non-basal slip and micro-kinking. By comparison with the structural rearrangement observed in the pre-annealed specimen, the laser damage zone showed only very retarded changes.

D FORM 1473  
1 NOV 65

Unclassified

Security Classification

AGO 5698A

14	KEY WORDS		LINK A		LINK B		LINK C	
	ROLE	WT	ROLE	WT	ROLE	WT	ROLE	WT
Laser induced damage X-ray diffraction Dislocation Zinc crystal								

Quarterly Technical Report  
For

Period March 22, 1971 to June 21, 1971

Submitted to the U. S. Army Research Office

ARPA	675, Am 9
Program Code Number:	9E20
Name of Grantee:	University of Maryland
Effective Date of Grant:	December 22, 1970
Grant Expiration Date:	December 21, 1971
Amount of Grant:	\$29,969
Principal Investigator and Phone Number:	Dr. Chi H. Lee (301) 454-2443
Grant Number:	DA-ARO-D-31-124-71-55 <sup>6</sup>
Project Scientist or Engineer:	None
Short Title of Work:	"The Study of the Interaction of Intense Picosecond Light Pulse with Materials"

Report by:

Chi-Hsing Lee

Dr. Chi H. Lee  
Assistant Professor

## Quarterly Technical Report

During this period we have spent considerable amount of effort to study the laser induced damage in single crystal which was initiated a few months ago. We shall concentrate our technical report for this quarter on this subject. The investigation was motivated by the frequent damage produced in the GaAs sample during the course of study on the two-photon photoconductivity effect. For a more comprehensive understanding of the damage process in material under laser radiation, we have chosen to collaborate with the material engineering group of the Engineering College at the University of Maryland. The Berg-Barrett x-ray diffraction contrast technique has been utilized to study the process of laser induced damage in a zinc crystal. It was found that the laser induced damage required a threshold energy which caused melting, possible vaporization and appreciable plastic deformation of the matrix material by deformation twinning, non-basal slip and micro-kinking. The preliminary result of this study is included in a paper entitled "Berg-Barrett X-ray Observation of Annealing and Laser Induced Damage in Zinc" which has been accepted for publication in the Journal of Applied Physics. The text of this report is just the reproduction of the paper cited.

**Berg-Barrett X-ray Observation of Annealing and  
Laser Induced Damage in Zinc**

by

**C.Cm. Wu<sup>\*</sup>, C.H. Lee<sup>+</sup> and R.W. Armstrong<sup>\*</sup>**

**\*Engineering Materials Group, and  
Department of Mechanical Engineering  
University of Maryland**

**<sup>+</sup>Department of Electrical Engineering  
University of Maryland**

# Berg-Barrett X-ray Observation of Annealing and Laser Induced Damage in Zinc

Carl Cm. Wu

Engineering Materials Group and Department of Mechanical Engineering  
University of Maryland

Chi H. Lee

Department of Electrical Engineering, University of Maryland

and

Ronald W. Armstrong

Engineering Materials Group and Department of Mechanical Engineering  
University of Maryland

The Berg-Barrett X-ray diffraction contrast technique has been utilized to study the process of laser induced damage in a zinc crystal and, also to make observations on the annealing characteristics of the dislocation substructure before and after the laser treatment. Annealing caused individual dislocations to become segmented with various sections of their line lengths becoming parallel to  $\langle 10\bar{1}0 \rangle$ . This preference for a crystallographic orientation of the dislocations seemed related to the equally important observation that the subboundary "lineage" structure of the crystals was also largely composed of tilt boundaries of  $\{10\bar{1}0\}$  and  $\{11\bar{2}0\}$  surfaces. The laser induced damage required a threshold energy which caused melting, possible vaporization and appreciable plastic deformation of the matrix material by deformation twinning, non-basal slip and micro-kinking. By comparison with the structural rearrangement observed in the pre-annealed specimen, the laser damage zone showed only very retarded changes.



## I. Introduction

The Berg-Barrett x-ray diffraction contrast technique<sup>1,2</sup> is established to be a particularly useful method for revealing directly individual dislocations and the dislocation substructure in zinc crystals<sup>3-8</sup>. Previous observations have shown that dislocations in zinc move easily at room temperature by climb and glide processes, partly because this temperature is a relatively high temperature, i.e. approximately 43% of the absolute melting temperature, and because zinc is relatively soft; the resolved shear stress for basal slip being approximately 25 grams/mm<sup>2</sup><sup>9-10</sup>.

The forgoing considerations led us to investigate whether the annealing process could be studied or any influence on the dislocation substructure could be produced by bombarding a specimen with a regulated pulse from a laser beam. The laser experiment offers the possibility of obtaining a controlled energy dissipation within a specific region of a crystal. Exceptional temperatures and pressures might be generated under appropriate conditions. The following is an account of our results.

## II. Experimental Procedure

The specimen studied was a section of an  $\{0001\}$  oriented zinc single crystal rod previously grown from the melt by the Bridgman technique, as reported elsewhere<sup>11</sup>. A tetragonal section of about 0.5 cm height was cleaved parallel to  $\{0001\}$  from a bar of square cross section, 1.0 cm<sup>2</sup>, at liquid nitrogen temperature.

Cobalt K $\alpha$  radiation from a Norelco sealed tube or a Jarrell-ash micro-focus unit was used to obtain  $\{10\bar{1}3\}$  Bragg reflections through the  $\{0001\}$  surface. The diffraction spots, of size nearly equal to the total surface area of the crystal, were recorded on Ilford 10 microns L-4 Nuclear plate or Kodak High Resolution plates. The tube was operated at 25KV and 15 ma for

the Norelco unit and 22 KV and 4 ma for the Jarrell-Ash unit. A layer of iron-oxide of 0.0025 inches thickness was placed between the plate and specimen surfaces. Exposure times ranged from 0.5 hour to 24 hours depending mainly on the sensitivity of each type of film (emulsion).

The laser was a Korad K-1 Nd: glass system passively Q-switched by a Kodak 9860 dye solution. The laser was used to bombard the specimen at a predetermined area with laser pulses of different energies, after which x-ray micrographs were obtained and examined. The size of the impacted area was approximately  $5.0 \text{ mm}^2$ . The maximum output of the laser pulse was about 0.2 joules in 60 nano-seconds. To deliver energies smaller than the full output of the system, neutral density filters were placed in the beam path. The laser pulse was monitored and its pulse width measured. Its wavelength is centered at 1.06 microns. The energy of the beam was measured by a thermopile.

### III Experimental Results

The dislocation structure observed within the subgrains of the freshly cleaved specimen is shown in Figure 1. The individual dark dislocation lines within the polygonal area KPGFA are revealed because of the enhanced x-ray intensity diffracted from their local vicinity. The sub-boundary structure outlining the individual subgrains is mainly revealed as a network of wide black or white bands, such as at KL and CA, respectively. This contrast is only an apparently increased or decreased x-ray intensity diffracted from the crystal, because it is actually caused by displacement of the diffracted intensity from either side of a boundary due to the relative misorientation of the subgrain volumes. The extinction contrast whereby individual dislocations are black and, separately, extinction plus misorientation contrast whereby subgrain boundaries are seen as black or white bands with occasional black edges has been previously described<sup>3</sup>.

The majority of the long dislocation lines in Figure 1 are aligned nearly parallel to  $[\bar{1}2\bar{1}0]$ . This was both the direction of cleavage for this crystal and also the trace of the diffracting plane in the cleavage surface. Both factors have been shown to be associated with the enhanced observation of these particular dislocation lines<sup>3,8</sup>. However, the principal crystallographic feature to be noted in Figure 1 is that a number of the dislocation subgrain boundaries are also parallel over appreciable portions of their lengths to specific crystal directions. For example, the boundary AE is parallel to  $[01\bar{1}0]$ , KC is parallel to  $[2\bar{1}\bar{1}0]$  and AD is parallel to  $[41\bar{5}0]$ . Kinks appear along the length of certain boundaries, such as at LM, ON and E, and even they appear to follow specific crystallographic directions. In certain places, such as at J, the dislocation density is sufficiently great that individual dislocations are not revealed but a general area of greatly enhanced intensity is observed.

Since annealing occurs easily at room temperature, the specimen shown in Figure 1 was set aside for a period of two weeks and then examined again. The result is shown for this identical region in Figure 2. The arrangement of individual dislocations is seen to be changed. A large number of the dislocations have become segmented with line lengths parallel to  $\langle 10\bar{1}0 \rangle$ . Note also the improved resolution. This was obtained largely by reducing the specimen-film distance, as can be surmised from the reduced width of the dislocation subboundaries, e.g. subboundary CA is approximately 50% narrower in Figure 2 than in Figure 1, and this means that the specimen-film distance has also been halved (to a value of 1.0 mm).

The influence of an impinging laser beam on the destruction of the crystalline perfection of the region shown in Figures 1 and 2 is shown in Figure 3. The incident laser pulse contained the maximum energy of 0.2 joules.

4.  
In some local regions of the area shown in Figure 3, the crystalline perfection is so distorted that the Bragg diffraction condition is no longer satisfied. This was indicated, also, by the appearance of the surface of the crystal when viewed in the optical microscope, as shown in Figure 4. It is evident from Figure 4 and from an even more detailed study of the surface that the crystal has been partially melted and the molten metal has been sprayed from the impact area. Several large deformation twins along  $\langle 2\bar{1}\bar{1}0 \rangle$  with parallel accommodation boundaries are recognizable in Figure 4 and are also detected by the absence of their Bragg reflection in Figure 3. Finer details are also revealed in Figure 3. Non-basal slip bands are observed in considerable amount though in diffuse contrast along  $\langle 10\bar{1}0 \rangle$ , such as at SQ. Also, a large amount of very localized black-white contrast effects are observed along  $\langle 10\bar{1}0 \rangle$ , such as at K and V. These effects are probably due to micro-kinking of the material. These latter deformation markings frequently form angular patterns in the x-ray micrographs. They are also detected with less obviousness in the optical microscope, as shown in Figure 4.

The influence of an annealing treatment on the damaged area is shown in Figure 5 which was taken eight months after the laser bombardment experiment. Some annealing has occurred. Within the laser impacted area KPGFA, it appears that less distortion is present because more of the impacted area appears to be diffracting x-rays again. However, in the vicinity of the area AEDB more significant rearrangement of the dislocation substructure is observed. While in Figure 3, this area appears to be generally distorted because of the diffuse enhanced intensity, it now can be seen that heavy bands of dislocation lines have appeared. Furthermore, they are also aligned reasonably parallel to  $\langle 10\bar{1}0 \rangle$ , which is similar to those lines observed in area KPGFA of Figure 2.

#### IV. Discussion:

It seems quite interesting that the crystal subboundaries have been observed to be largely composed of straight segments which produce traces in the (0001) that are parallel to specific crystallographic directions, e.g. of type  $\langle 10\bar{1}0 \rangle$ ,  $\langle 11\bar{2}0 \rangle$ , and other higher index types. This observation has not been previously reported. Since the crystal has been solidified along the [0001], it follows that the subboundaries form a lineage structure<sup>12</sup>. Thus, the boundaries contain the crystal growth direction, and, therefore, an  $[01\bar{1}0]$  boundary trace corresponds to a  $(2\bar{1}\bar{1}0)$  subboundary orientation. The vertical white boundary AF in Figure 1 has this orientation and, because of the (under lapping) constant subboundary width along its length, the indication is that the boundary must be a pure tilt boundary with rotation around  $[01\bar{1}0]$  contributed by dislocations with Burgers vector along  $[2\bar{1}\bar{1}0]$ . The narrow black extinction band observed at certain positions on either side of AF is attributed to the very localized nature of the boundary strains due to the compensatory overlapping of the individual dislocation strain fields. This explanation is seen to be correct by comparison of this narrow extinction band with the wider ones due to the parallel individual dislocations within the subgrain volume.

The kinked segments LMNO along the boundary KP present a special situation. In the first instance, the boundary width along the segment KP is not nearly so different between Figures 1 and 2 as applies for AF and, therefore, it might be imagined that the misorientation or extinction contrast of KP is not very simple. In fact, the kink boundary segment along KP was observed in the optical microscope to exhibit due to slightly varying surface tilts a straight boundary segment directly connecting LO. The absence of any boundary contrast in the x-ray micrographs strongly implies that the misorientation

associated with L0 must be due to a rotation about the normal to  $(10\bar{1}3)$  - the diffracting plane - and/or that the dislocation Burgers vectors associated with the actual rotation should be contained within the diffracting plane. The nearly equal extinction and misorientation contrast associated with the kink segment NO in Figure 2 could be explained by a tilt boundary rotation about  $[\bar{1}100]$  due to  $[11\bar{2}0]$  Burgers vector dislocations. This latter misorientation and extinction contrast appears consistent, also, with the contrast appearance of the remaining segments of the total boundary running along KLMN and OP, whereby the extinction contrast merely outweighs the misorientation contrast.

The individual dislocation lines within the subgrains of the freshly cleaved crystal are long and aligned parallel to the cleavage direction as reported previously<sup>8</sup>. Due to normal room temperature annealing of the cleaved crystal surface, these dislocation lines moved about and straightened themselves. The annealed structure is composed of segmented dislocation lengths lying along  $\langle 10\bar{1}0 \rangle$  directions and is in fact similar to the structures observed by Michell and Ogilvie<sup>13</sup> in vapor condensed specimens, even though the dislocations observed by Michell and Ogilvie were freshly nucleated within the crystal after the specimen was exposed to room temperature (annealing) for a lengthy time period. Nevertheless, the dislocations observed in Figure 2 are considered to be a rearrangement of either some of those dislocations introduced during cleaving or those originally present in the specimen.

The generally small amount of dislocation rearrangement due to annealing of the laser impacted specimen after even eight months at room temperature leads us to look for some reason for the deformation state to be "locked-in". For example, the damaged area might be covered by a thin film of fine grained

polycrystalline material which might act to retard changes in the defect structure. The rearrangement of the dislocations which has occurred does seem to follow the pre-annealed pattern of changes, i.e. the dislocations move about to align themselves approximately parallel to  $\langle 10\bar{1}0 \rangle$ . No doubt, the preference of individual dislocations to be along  $\langle 10\bar{1}0 \rangle$  carries over to explain the similar preference for the principal subboundaries to also lie along these directions.

At this point it should be pointed out that the bombardment of this specimen with laser pulses of gradually increasing energy through  $10^{-4}$ ,  $10^{-3}$  and  $2 \times 10^{-2}$  joules prior to the 0.2 joule impacting did not cause any observable change in the crystal, as measured with the optical microscope or by x-ray diffraction micrographs. In this regard, the incident energy of 0.2 joules which, say, might potentially be dissipated within a volume of area  $5.0 \text{ mm}^2$  by  $10^{-3}$  mm depth gives an energy density of  $4 \times 10^{11} \text{ dynes/cm}^2$ . This energy density, which obviously exceeded any threshold value for damage of the zinc (0001) surface layer may be compared with various energy density or stress values given for melting, vaporization, twinning, slip, kinking or forming new surface area in zinc, as specified in Table 1. From the Table it may be seen that the impacting energy density exceeds but is comparable to, the total energy density required to vaporize zinc atoms. However the energy density present within the  $2 \times 10^{-2}$  joule beam should have been sufficient to melt the crystal also, but this did not occur, so that only on the order of 10% or so of the incident energy must have been absorbed in that impacting process. On this basis without allowing for any non-linear absorption effects, it may be estimated that an absorbed energy density equal to or less than  $4 \times 10^{10} \text{ dynes/cm}^2$  is required to cause damage in zinc. This energy density exceeds by far

the elastic stress values, and accompanying far lesser strain energy values, associated with the various deformation mechanisms shown in Table 1. Consequently, it may be imagined that the deformation which has occurred in the damage process represents a minor part of the total damage itself, say, by being produced by the thermal stresses accompanying the very rapid process of melting and even superheating, an amount of liquid zinc at the crystal surface. This concern for the importance of thermal stresses in evaluating the performance of laser materials themselves has been recently emphasized<sup>17</sup>.

#### V. Summary

Specific characteristics of individual dislocations, dislocation subboundaries, and laser induced damage in a cleaved zinc specimen have been revealed by the Berg-Barrett x-ray diffraction micrographic method:

1. The dislocations in the freshly cleaved specimen appeared as long lines roughly aligned parallel to the cleavage direction and then, following room temperature annealing, they became segmented and aligned themselves more sharply parallel to  $\langle 10\bar{1}0 \rangle$ .
2. The dislocation subboundaries, which were present within the crystal as the lineage structure, were also observed to be aligned parallel to low index directions, e.g. several of the subboundaries were observed to be pure tilt boundaries contained within  $\{10\bar{1}0\}$  and  $\{11\bar{2}0\}$ .
3. The laser induced damage seemed to have required a threshold energy which caused melting, possible vaporization, deformation twinning, slip, and micro-kinking, all of which appeared to have combined to produce a damage zone that showed very retarded changes by annealing (in comparison with the structural rearrangements observed in the pre-annealed specimen).



An assessment of the energy density in several laser impacts gave, in comparison with tabulated values of energy densities and stresses for structural changes in zinc, an indication that all of the features of the damage zone followed on from the melting and, at least, superheating of a liquid film on the specimen surface.

#### Acknowledgment

This research was supported by the Advanced Research Projects Agency through the Center of Materials Research and through Contract DA-ARD-D-31-124-70G50 (monitored by the Army Research Office). The authors are grateful to Professors B. Roessler and S.J. Burns of Brown University for helpful discussions.

## References

1. C.S. Barrett, Trans. AIME 161, 15, (1945).
2. J.B. Newkirk, Trans. AIME 215, 483, (1959).
3. J.M. Schultz and R.W. Armstrong, Phil. Mag. 10, 497, (1964).
4. J.M. Schultz and R.W. Armstrong, Acta Met. 14, 436, (1966).
5. J.M. Schultz and R.W. Armstrong, Surface Sci. 12, 19, (1968).
6. R.W. Armstrong, Phys. Stat. Sol. 11, 355, (1965).
7. D.P. Pope, T. Vreeland and D.S. Wood, J. Appl. Phys. 38, 4011, (1967).
8. S.J. Burns, Acta Met. 18, 969, (1970).
9. D.C. Jillson, Trans. AIME 188, 1005, (1950).
10. S. Harper and A.H. Cottrell, Proc. Phys. Soc. B63, 331, (1950).
11. J.M. Schultz and R.W. Armstrong, "Direct Observation of Imperfections in Crystals" (Interscience: New York), p. 569, (1962).
12. B. Chalmers, "Physical Metallurgy", (John Wiley and Sons; New York), p. 259, (1959).
13. D. Michell and G.J. Ogilvie, Phys. Stat. Sol. 15, 83, (1966).
14. R.L. Bell and R.W. Cahn, Proc. Roy. Soc. A239, 494, (1957).
15. J.J. Gilman, Trans. AIME, 203, 206, (1955).
16. W.A. Miller, G.J.C. Carpenter and G.A. Chadwick, Phil. Mag. 19, 305, (1969).
17. H.S. Bennett, J. Appl. Phys. 42, 619, (1971).

Table Caption

Table 1. Energy Densities and Stresses for Laser Induced Damage in Zinc

Table 1. Energy Densities and Stresses for Laser Induced Damage in Zinc

Material Property	Energy density or Stress Value	Reference
Heat of fusion per unit volume	$7.3 \times 10^9$ dynes/cm <sup>2</sup>	Hdbk. Chem. Phys. (1970)
Heat of vaporization per unit volume	$1.3 \times 10^{11}$ dynes/cm <sup>2</sup>	Hdbk. Chem. Phys. (1970)
Resolved shear stress for $\{10\bar{1}2\}\langle 10\bar{1}1 \rangle$ twinning	$3.2 \times 10^8$ dynes/cm <sup>2</sup>	Bell and Cahn (1957) <sup>14</sup>
Resolved shear stress for $\{11\bar{2}2\}\langle 11\bar{2}3 \rangle$ slip	$1.3 \times 10^8$ dynes/cm <sup>2</sup>	Bell and Cahn (1957) <sup>14</sup>
Compressive stress for $\{10\bar{1}0\}\langle 11\bar{2}0 \rangle$ kink	$1.7 \times 10^8$ dynes/cm <sup>2</sup>	Gilman (1955) <sup>15</sup>
Resolved shear stress for $\{0001\}\langle 11\bar{2}0 \rangle$ slip	$1.8 \times 10^6$ $3.4 \times 10^6$ dynes/cm <sup>2</sup>	Jillson (1950) <sup>9</sup> Harper and Cottrell (1950) <sup>10</sup>
Surface energy per atomic (c) distance	$2.3 \times 10^{10}$ dynes/cm <sup>2</sup>	Miller, Carpenter and Chadwick (1969) <sup>16</sup>

### Figure Captions

- Figure 1. X-ray micrograph of  $\{0001\}$  surface of an as cleaved zinc single crystal;  $(10\bar{1}3)$  reflection, Co-K $\alpha$  radiation. Dislocations (black wavy lines along  $[\bar{1}2\bar{1}0]$ ) and dislocation subboundaries (AB, AC, AF, etc.) are seen. 65X.
- Figure 2. Same area as Figure 1, after the specimen was annealed at room temperature for two weeks. The dislocation arrangement has changed from that shown in Figure 1 due to the annealing process. The dislocations have become segmented along  $\langle 10\bar{1}0 \rangle$ . 65X
- Figure 3. Same area as Figures 1 and 2, after specimen was damaged by an impinging laser beam. Twins (such as at TW and IN) slip bands (such as SQ), and micro-kinking (such as at V and Z) have occurred.
- Figure 4. Optical micrograph of the damaged area shown in Figure 3. The damage area has been melted by the impact and molten metal has been sprayed from the area.
- Figure 5. Same area as Figures 1, 2 and 3, after eight months since damage occurred. Only retarded annealing is observed in the damage area. Rearrangement of non-basal slip dislocations is observed.



Figure 1. X-ray micrograph of (0001) surface of an as cleaved zinc single crystal;  $(10\bar{1}3)$  reflection, Co- $K\alpha$  radiation. Dislocations (black wavy lines along  $[\bar{1}2\bar{1}0]$ ) and dislocation subboundaries (AB, AC, AF, etc.) are seen. 65X.

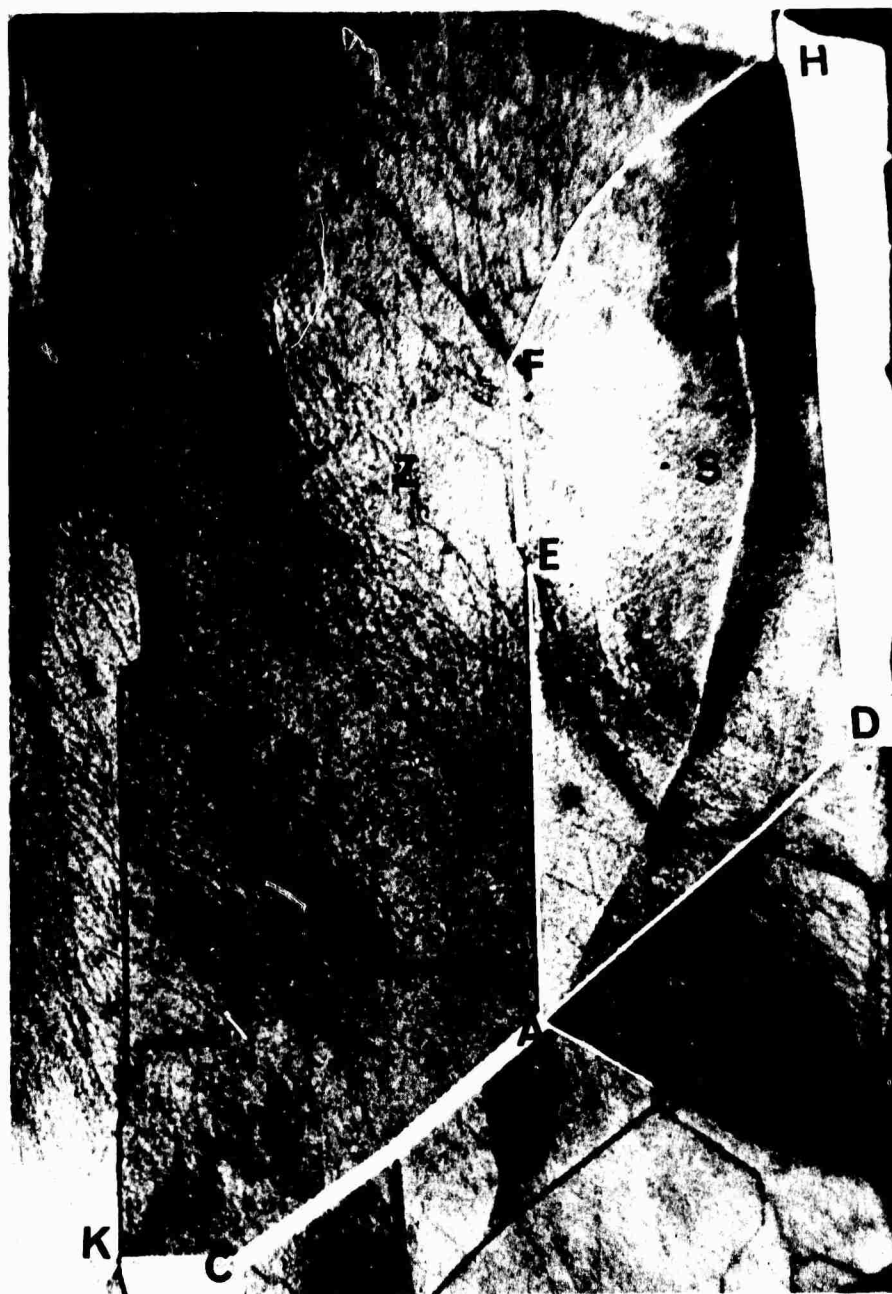


Figure 2. Same area as Figure 1, after the specimen was annealed at room temperature for two weeks. The dislocation arrangement has Changed from that shown in Figure 1 due to the annealing process. The dislocations have become segmented along  $\langle 10\bar{1}0 \rangle$ . 65X



Figure 3. Same area as Figures 1 and 2, after specimen was damaged by an impinging laser beam. Twins (such as at TW and IN) slip bands (such as SQ), and micro-kinking (such as at V and Z) have occurred.





Figure 4. Optical micrograph of the damaged area shown in Figure 3. The damage area has been melted by the impact and molten metal has been sprayed from the area.

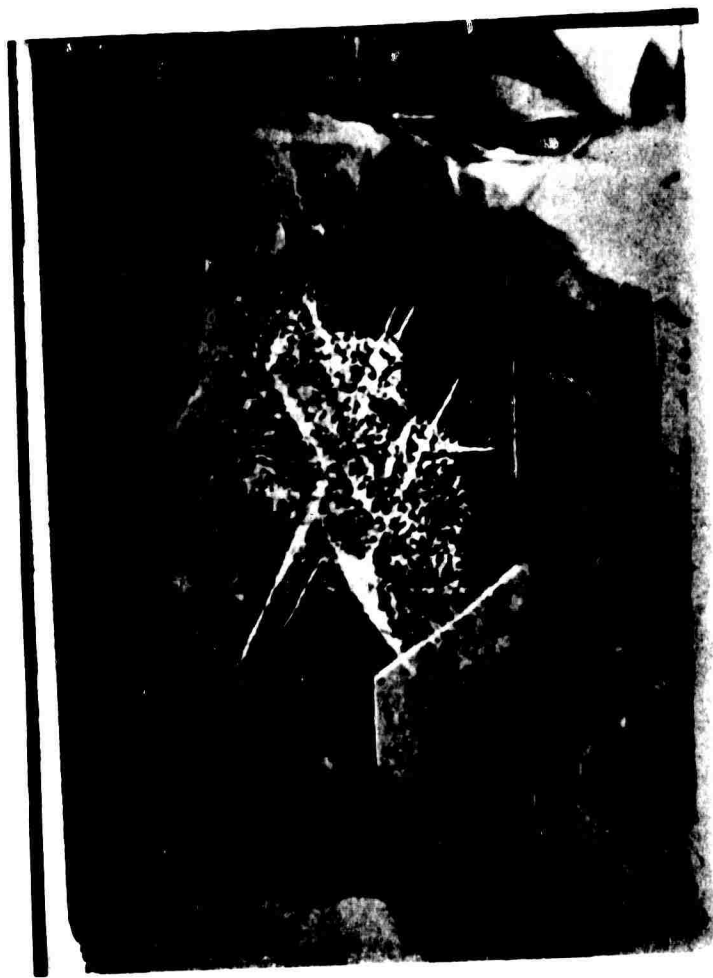


Figure 5. Same area as Figures 1, 2 and 3, after eight months since damage occurred. Only retarded annealing is observed in the damage area. Rearrangement of non-basal slip dislocations is observed.